Expanded View Figures

Figure EV1. Loss of Grp1 causes defects in cell growth.

A Hyphal form (6 hours post-induction, h.p.i.) of laboratory strain AB33 expressing a Gfp-tagged protein with nuclear localisation signal to stain the nucleus (N; λN-NLS-Gfp, phage protein λN fused to triple Gfp, containing a nuclear localisation signal; inverted fluorescence image shown; scale bar, 10 μm). Hyphae expand at the apical pole (arrow) and insert septa (asterisks) at the basal pole in regular time intervals resulting in the formation of empty sections.

B Schematic representation of the domain architecture of four small glycine-rich proteins (RRM, RNA recognition motif, green; GQ/R, glycine-rich region with arginine or glutamine, red). *Um*Grp1 from *U. maydis* (UMAG_02412), *At*GRP7 from *Arabidopsis thaliana* (RBG7; NC_003071.7), *Hs*RBM3 and *Hs*CIRBP from *Homo sapiens* (NC_000023.11 and NC_000019.10, respectively). Number of amino acids indicated on the right.

C Results of preliminary affinity purification experiments using Rrm4-GfpTT as bait (see Materials and Methods). Proteins with a functional link to Rrm4 are marked in red (this study) [18,64]. Peptide count: number of identified peptides corresponding to predicted protein; total peptide score: sum of all peptide scores corresponding to predicted protein, excluding the scores of duplicate matches; best peptide score: best score from all identified peptides corresponding to predicted protein. Note that the difference between total peptide score and best peptide score is a correction of the software depending on how many possible predicted candidates match to the identified peptide mass.

D Tandem affinity purification using Rrm4-GfpTT as bait. Protein bands were stained with Coomassie blue after SDS–PAGE. Proteins in boxed areas were identified as Rrm4 and Grp1 (size of marker proteins in kDa on the right).

E Growth curve of indicated AB33 derivatives growing in liquid culture. Data points represent averages from three independent experiments (n = 3). Error bars show s.d.

F Differential interference contrast (DIC) images of AB33 derivatives as yeast-like budding cells (scale bar, 10 μm).

G Length of budding cells (shown are merged data from three independent experiments, n = 3; > 100 cells per strain were analysed, *ωt*, 269; *rrm4Δ*, 122 (only two independent experiments); *grp1Δ*, 263; *grp1G*, 318), overlaid with the mean of means, red line and s.e.m.; paired two-tailed Student's t-test on the mean cell lengths from the replicate experiments.

H Colonies of indicated AB33 strains grown in the yeast form incubated at different temperatures (28°C for 1 day or 16°C and 21°C for 5 days).

I Colonies of indicated AB33 strains grown in the yeast form. Incubated plates contained cell wall inhibitors (CM, complete medium for 1 day; CFW, 50 μM calcofluor-white for 4 days; CR, 57.4 μM Congo red for 4 days).

J Fluorescence images of the basal pole of hyphae of AB33 derivatives (6 h.p.i.). Septa (asterisks) were stained with CFW. White bars indicate exemplary length measurements of empty sections shown in Fig 1D (scale bar, 10 μm).

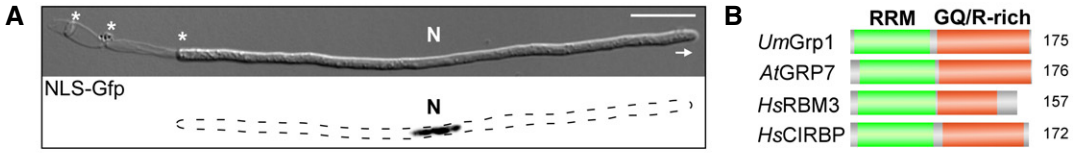

C

Nr.	UMAG	Annotation	MW[a]	PC[b]	Total PS[c]	Best PS[d]
1	10836	Rrm4	85	24	3086,8	252,7
2	11918	conserved hypothetical protein	95	4	582,2	196,6
3	10419	chitinase Cts1	55	5	513,1	130,3
4	06140	related to programmed cell death protein (calcium-binding protein)	34	4	457,7	182,1
5	05365	probable protein phosphatase 2A regulatory B subunit	53	3	322,4	124,2
6	10526	probable SSB2 - heat shock protein of HSP70 family, cytosolic	68	2	144,6	98,8
7	04080	probable DED1 - ATP-dependent RNA helicase	71	1	87,1	89,6
8	05158	related to Nucleoporin nup189 (SonB)	229	1	76,1	80,1
9	10350	Upa2	232	2	75,2	47,3
10	03791	Ums2heat shock 70 kd protein 2	70	1	71,4	73,9
11	**02412**	**Grp1, related to CIRBP - glycine-rich RNA-binding protein**	**18**	**1**	**68,8**	**71,3**
12	11551	probable 40S small subunit ribosomal protein S19	18	1	66,9	66,9
13	04619	related to HSE1, binds ubiquitin, mediates endosomal protein sorting	66	1	61,7	64,3
14	11211	Cutinase	51	1	59,3	63,3
15	01227	hypothetical protein	88	2	57,3	40,4
16	11719	probable ribosomal protein S4.e, cytosolic	30	1	56,9	59,4
17	06404	probable thioredoxin peroxidase	25	1	54,0	54,0
18	10163	probable 60S large subunit ribosomal protein L20	20	1	53,2	55,7
19	03738	probable ATP dependent RNA helicase	250	2	51,7	32,2
20	01077	putative protein	76	1	50,9	55,9
21	02578	related to Het-c heterokaryon incompatibility protein	108	2	50,0	31,9
22	01434	Fer3 siderophore peptide synthetase, ferrichromeA biosynthesis	528	2	46,8	31,3
23	01702	conserved hypothetical protein	20	1	46,2	46,2

[a] molecular weight [kDa]; [b] peptide count; [c] total peptide score; [d] best peptide score

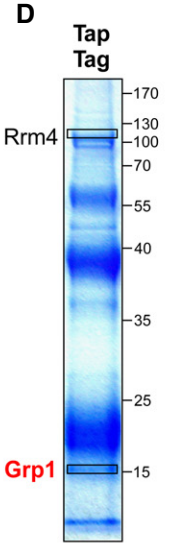

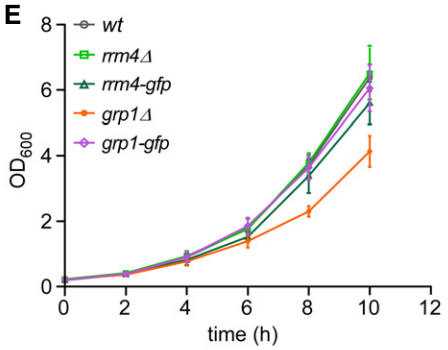

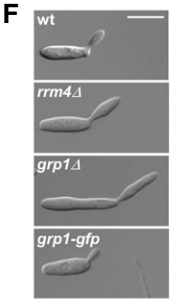

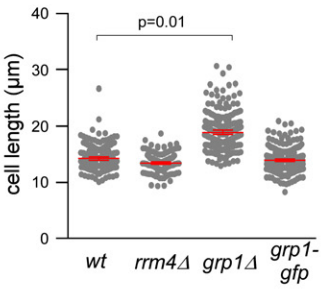

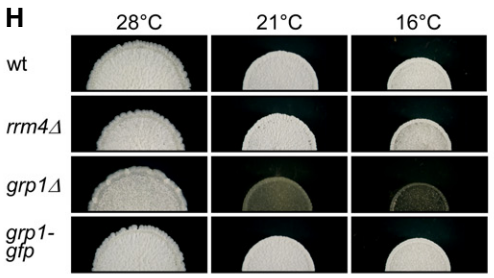

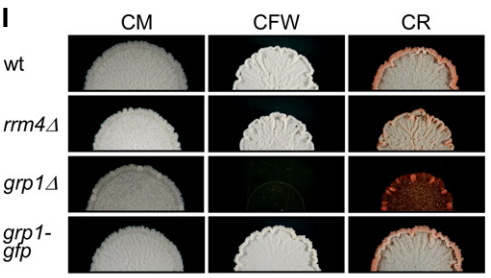

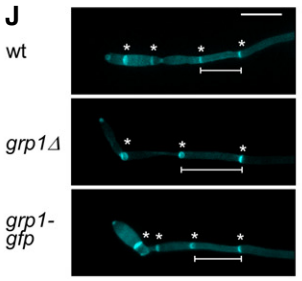

Figure EV1.

Figure EV2. Improving the iCLIP protocol for fungal RBPs.

A Grp1-Gfp/RNA complexes were size-separated on denaturing PAGE after UV-C irradiation and transferred to a nitrocellulose membrane (left). RNA was radioactively labelled, and protein-RNA complexes with covalently linked RNAs of different sizes were visible as smear above the expected molecular weight of the Grp1-Gfp protein (45 kDa; marked by arrowhead). RNA of four different regions of the membrane (A–D indicated on the right) were isolated from the membrane and were size-separated on a denaturing gel (6%) (right; nucleotide size marker on the left, bp).

B Autoradiographs showing Rrm4-Gfp, Grp1-Gfp and Gfp in complex with RNA after UV-C irradiation at 0, 160, 320, 480 and 640 mJ/cm^2. Corresponding Western blots using anti-Gfp are shown below. Arrowheads indicate the expected molecular weight of the proteins (Rrm4-Gfp, 112 kDa; Grp1-Gfp, 45 kDa; Gfp, 27 kDa). After each irradiation step, the cells were mixed. Note that increased UV-C irradiation in combination with slow processing due to long time intervals was particularly harmful to the Rrm4 protein, which was completely degraded after four minutes of UV-C irradiation. Putative degradation products are marked by asterisks.

C Autoradiographs showing Rrm4-Gfp, Grp1-Gfp and Gfp in complex with RNA after single UV-C irradiation at 0, 100, 200, 300 or 400 mJ/cm^2. This time, mixing breaks were omitted and cells were harvested as quickly as possible. Corresponding Western blots are shown below. Labelling as above. We chose 200 mJ/cm^2 as optimal UV-C irradiation dose, since the amount of unspecific Gfp-RNA complexes increased at higher doses. Arrowheads and asterisks as in (B).

D Amplification of the Rrm4-, Grp1- and Gfp-derived cDNA libraries with different numbers of PCR cycles (between 18 and 24; ctrl, control without template cDNA). The PCR products were separated on a native gel (6%) and stained with SYBR green I (nucleotide size marker on the left, bp). The size of the cDNA insert together with the adapters (cDNA insert = 20–30 nt; L3 adapter, RT-primer and P3/P5 Solexa primers = 128 nt) is expected to be ~ 150–160 nt after amplification.

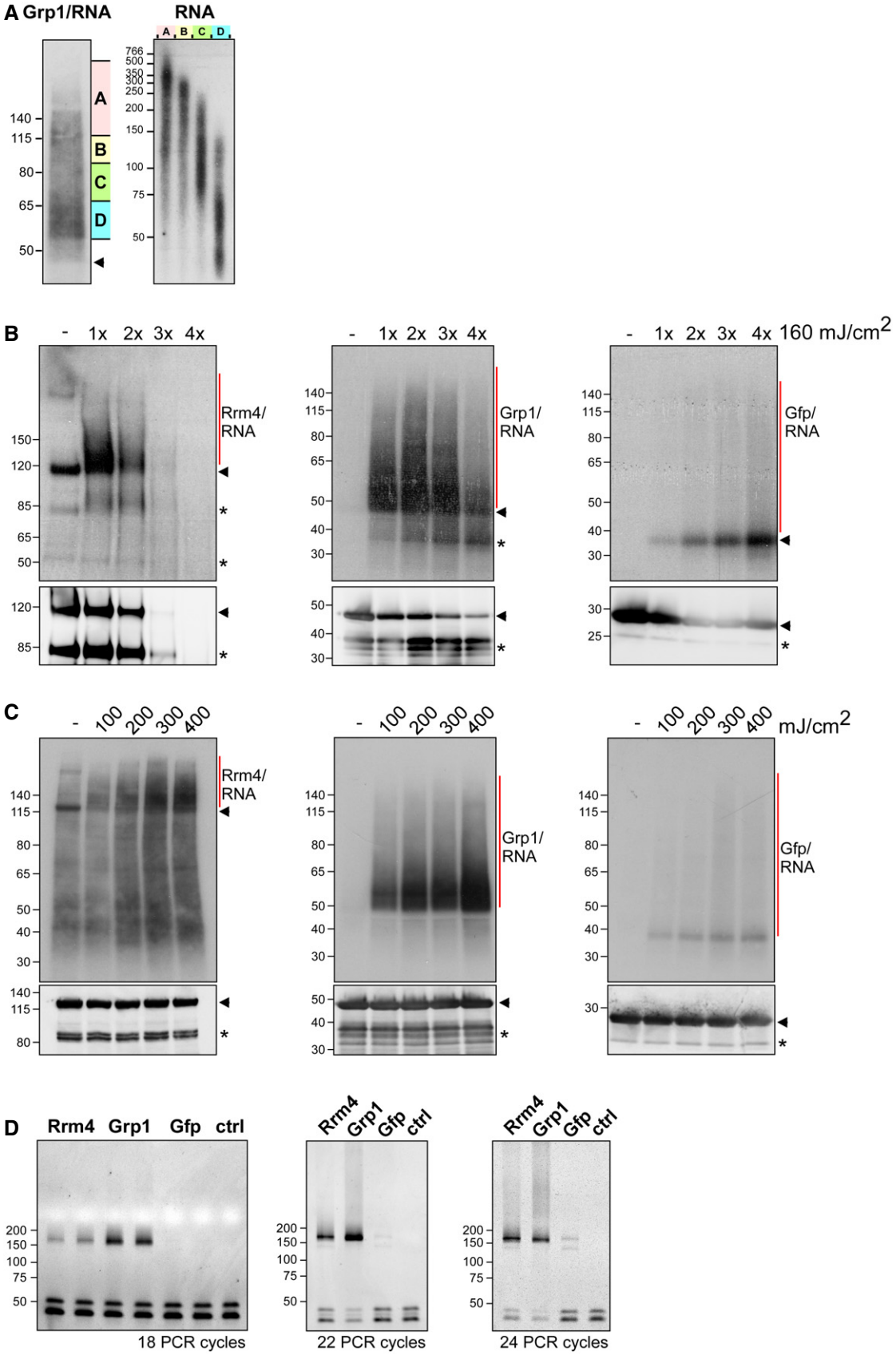
A Grp1/RNA
RNA
A
B
C
D
140
115
80
65
50
766
500
350
300
250
200
150
100
75
50
B
- 1x 2x 3x 4x
Rrm4/ RNA
Grp1/ RNA
Gfp/ RNA
160 mJ/cm2
150
120
85
65
50
40
30
25
C
- 100 200 300 400
mJ/cm2
D
Rrm4 Grp1 Gfp ctrl
200
150
100
75
50
18 PCR cycles
22 PCR cycles
24 PCR cycles

Figure EV2.

Figure EV3. Comparative iCLIP procedure results in high-quality dataset.

A Summary of the iCLIP libraries including initial number of sequencing reads, uniquely mapped reads, crosslink events (xlinks) for both replicates for Rrm4, Grp1 and Gfp. In addition, sum of crosslink events as well as resulting binding sites and target transcripts is given for merged replicates. Gfp binding sites were only filtered for reproducibility but not for relative signal intensity (SOB; see Materials and Methods).

B Stacked bar chart showing percentage of reads mapping to a unique, multiple (multiple mapping) or no location (unmapped) in the *U. maydis* genome for Rrm4, Grp1 and Gfp.

C Scatter plot comparing number of crosslink events per gene from two independent replicate experiments for Rrm4, Grp1 and Gfp (PCC, Pearson correlation coefficient).

D Genome browser views of Rrm4 and Grp1 iCLIP events as well as RNASeq data of *cts1* (UMAG_10419) and *rrm4* (UMAG_10836). Visualisation as in Fig 3C.

E Venn diagram to identify target transcripts that are uniquely bound by Rrm4 (left) or Grp1 (right). Unique target transcripts (numbers given in bold) are selected only if they show no evidence of binding by the other RBP (considering all binding sites before SOB filtering, see Materials and Methods).

A

		reads	uniquely mapped	crosslink events	Σ crosslink events	binding sites	genes
Rrm4	replicate1	14,791,625	9,027,052	2,777,064	4,683,060	6,412	3,262
	replicate2	24,757,620	16,269,064	1,905,996			
Grp1	replicate1	41,915,499	26,716,134	9,106,077	14,789,890	6,478	3,165
	replicate2	18,157,540	12,288,327	5,683,815			
Gfp	replicate1	671,922	208,847	73,398	153,851	NA	59*
	replicate2	2,262,880	885,903	80,453			

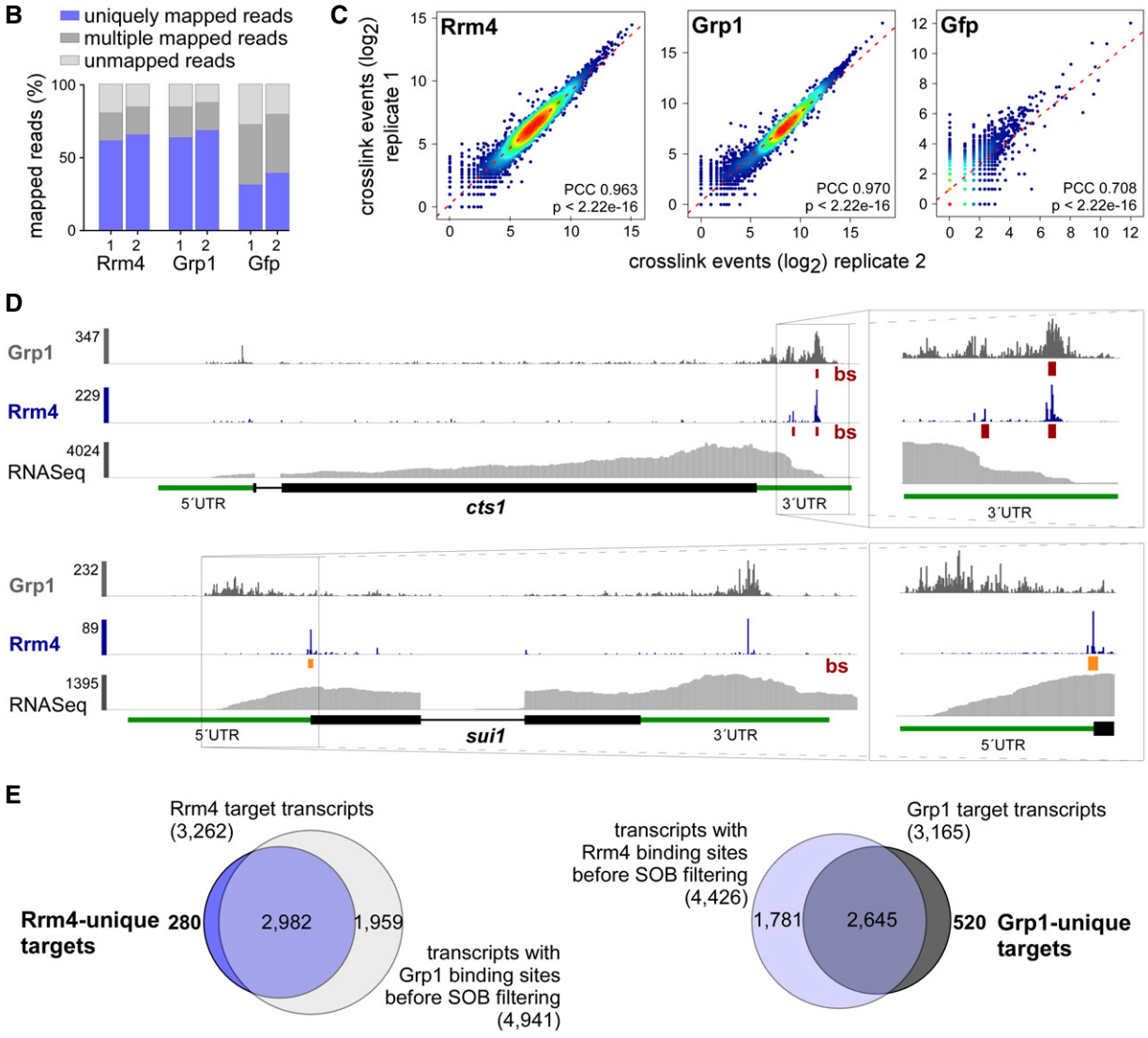

Figure EV3.

Figure EV4. Accumulation of crosslink events at stop codons of mRNAs encoding subunits of the mitochondrial F_1F_O-ATPase.

A Heatmap of crosslink events of Grp1 (left) and Rrm4 (right) in a window around the stop codons (position 0 = first position of 3′ UTR) of mRNAs encoding subunits of the mitochondrial F_1F_O-ATPase (nomenclature and gene identifiers for *U. maydis* on the right). Crosslink events per nucleotide are represented by a colour scale (right).

B, C iCLIP data of Rrm4 and Grp1 as well as RNASeq data across selected mRNAs of the F_1 subcomplex (B) and F_O subcomplex (C) that carry an Rrm4 binding site precisely at the stop codon. Visualisation as in Fig 3C.

D Cy2 image of a representative differential gel electrophoresis (DIGE) analysis comparing membrane-associated proteins of wild type (blue, Cy5-labelled) and *rrm4Δ* hyphae (red, Cy3-labelled; size marker on the left, pH range at the top; 6 h.p.i.). Protein variants exhibiting at least 2.5-fold differences in protein amounts are indicated by numbered arrowheads (taken from earlier study) [18]. The area marked with a yellow rectangle is enlarged on the right. The corresponding standardised logarithmic protein abundances for the Atp4 spot obtained from three biological replicates are given on the right (internal standard set to 0).

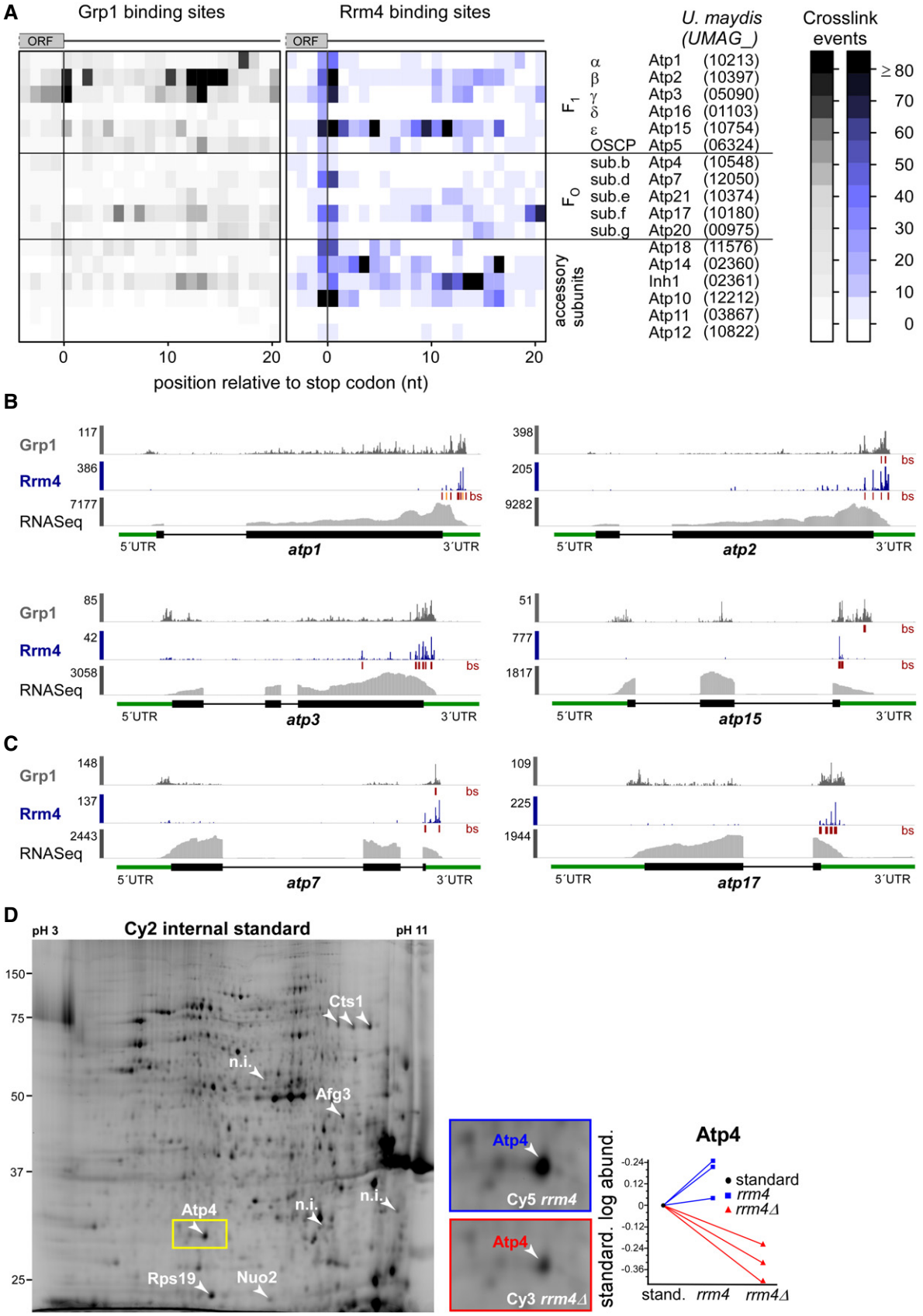
A
Grp1 binding sites
Rrm4 binding sites
ORF
ORF
U. maydis (UMAG_)
Crosslink events
F1
α Atp1 (10213)
β Atp2 (10397)
γ Atp3 (05090)
δ Atp16 (01103)
ε Atp15 (10754)
OSCP Atp5 (06324)
FO
sub.b Atp4 (10548)
sub.d Atp7 (12050)
sub.e Atp21 (10374)
sub.f Atp17 (10180)
sub.g Atp20 (00975)
accessory subunits
Atp18 (11576)
Atp14 (02360)
Inh1 (02361)
Atp10 (12212)
Atp11 (03867)
Atp12 (10822)
≥ 80
70
60
50
40
30
20
10
0
0
10
20
0
10
20
position relative to stop codon (nt)
B
Grp1
Rrm4
RNASeq
117
386
7177
bs
5´UTR
atp1
3´UTR
398
205
9282
bs
5´UTR
atp2
3´UTR
85
42
3058
bs
5´UTR
atp3
3´UTR
51
777
1817
bs
5´UTR
atp15
3´UTR
C
148
137
2443
bs
5´UTR
atp7
3´UTR
109
225
1944
bs
5´UTR
atp17
3´UTR
D
pH 3
Cy2 internal standard
pH 11
150
75
50
37
25
Cts1
n.i.
Afg3
n.i.
n.i.
Atp4
Rps19
Nuo2
Atp4
Cy5 rrm4
Atp4
Cy3 rrm4Δ
standard. log abund.
Atp4
0.24
0.12
0
-0.12
-0.24
-0.36
standard
rrm4
rrm4Δ
stand.
rrm4
rrm4Δ

Figure EV4.

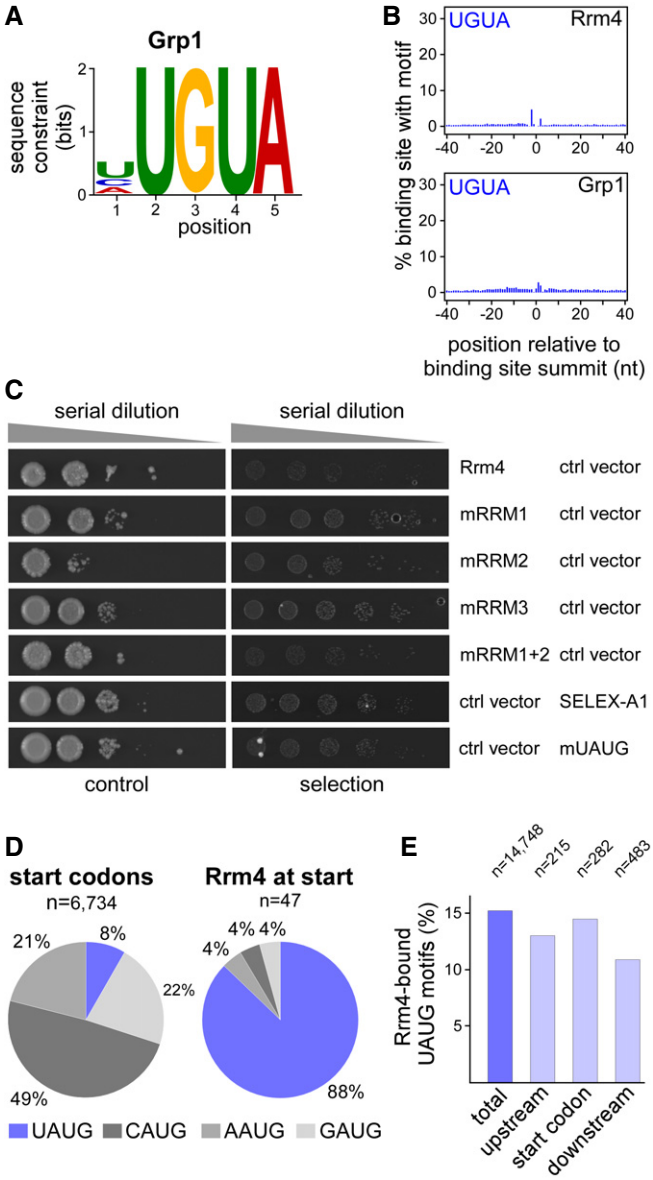

Figure EV5. Control experiments for the yeast three-hybrid analysis.

A Logo representation of the most enriched sequence motif at Grp1 binding sites. At each position, the height of the stack is proportional to the information content, while the relative height of each nucleotide within the stack represents its relative frequency at this position.

B Frequency of UGUA around Rrm4 and Grp1 binding sites. Shown is the percentage of binding sites that harbour an UGUA starting at a given position in an 81-nt window around the binding site summit. Representation as in Fig 5B.

C Colony growth on control and selection plates of yeast cells expressing protein and RNA hybrids indicated on the right. RNA binding is scored by growth on selection plates (SC –his +3-AT, 3-amino-1,2,4-triazole). This control experiment demonstrates that growth on selection plates (see Fig 5F) depends on the presence of Rrm4 variant and cognate hybrid RNA. mRRMx, Rrm4 variants harbouring mutations in RRM 1, 2, 3 or 1 and 2.

D Relative occurrence of NAUG sequence context for all (left) and Rrm4-bound (right) start codons. CAUG fits to the Kozak sequence in eukaryotes [81]. The fraction of start codons coinciding with the Rrm4 recognition motif UAUG is shown in blue. This sequence context was strongly enriched among the Rrm4-bound target mRNAs, whereas it comprises only 8% of all annotated start codons in the *U. maydis* genome.

E UAUG motifs at start codons were not more frequently bound than UAUG motifs in the surrounding sequence (see Materials and Methods). Out of a total of 14,748 UAUG motifs in expressed transcripts, 15.2% are bound by Rrm4. Similarly, 14.5% of the 282 UAUG motifs directly at start codons are bound by Rrm4. This is only marginally more than at 215 and 483 UAUG motifs within 100-nt upstream and downstream of the start codons, out of which 13.0% and 11.0% are bound, respectively.